A DESIGN APPROACH FOR SUPERCONDUCTING HIGH-CURRENT ION LINACS

R. W. Garnett and T. P. Wangler
Accelerator Operations and Technology Division
Los Alamos National Laboratory
Los Alamos, New Mexico 87545, USA*

Abstract

An approach for designing superconducting high-current ion linacs is described. This approach takes advantage of the large velocity acceptance of high-gradient cavities with a small number of cells. It is well known that this feature leads to a linac design with great operational flexibility. Algorithms which have been incorporated into a design code and a beam dynamics code are discussed. Simulation results using these algorithms are also presented.

Introduction

The work presented here is part of an ongoing effort [1] to design reliable, low-loss, high-current, cw superconducting ion linacs for applications such as accelerator transmutation of waste, the next generation spallation neutron sources, and accelerator production of tritium. We have limited our effort to the design and simulation of a 100-1000 MeV, 100mA, cw linac which uses independently-phased elliptical multicell superconducting rf cavities to accelerate a proton beam. However, our approach should be more generally applicable. The expressions presented below can be used to determine the linac cavity parameters such as the number of cells/cavity, the velocity range over which a cavity can efficiently accelerate beam, and the required cavity gradient.

Our approach takes advantage of the large velocity acceptance of high-gradient superconducting cavities. An analytic model of multi-cell elliptical cavities excited in a π-mode was used to determine the initial cavity parameters. A simple cavity field distribution was assumed where the fields are uniform in the gaps and fall to zero immediately outside the gaps. With this assumption, an approximate expression for the transit-time factor T can be given as a product of two separate factors $T = T_G T_S$. The gap factor T_G is the transit time for a gap of length g and is given by the expression $T_G = \sin(\pi g/\beta\lambda)/(\pi g/\beta\lambda)$. The synchronism factor T_S, is a function of the number of cells per cavity N and of the ratio of the reference-particle velocity, β, to the cavity geometric velocity, β_G. The synchronism factor is given by:

$$T_S(N,\beta/\beta_G) = \begin{cases} (-1)^{(N-1)/2}\cos(N\pi\beta_G/2\beta)/N\cos(\pi\beta_G/2\beta), N-odd \\ (-1)^{(N/2+1)}\sin(N\pi\beta_G/2\beta)/N\cos(\pi\beta_G/2\beta), N-even \end{cases} \quad (1)$$

where $g = \beta_G\lambda/2$. Figure 1 shows the model predictions for the transit-time factor T for various numbers of cells/cavity as a function of the ratio β/β_G. In order to choose the number of cells per cavity, a compromise must be made between many competing effects. As can be seen in the figure, a small number of cells/cavity provides a large velocity acceptance. Additionally, the power-coupler levels, for a given beam current and field, are lower and the cavity field uniformity is easier to maintain. Using a larger number of cells has the advantage of reducing the overall number of system components, system size, and system complexity. In our design example, we have chosen 4 cells/cavity.

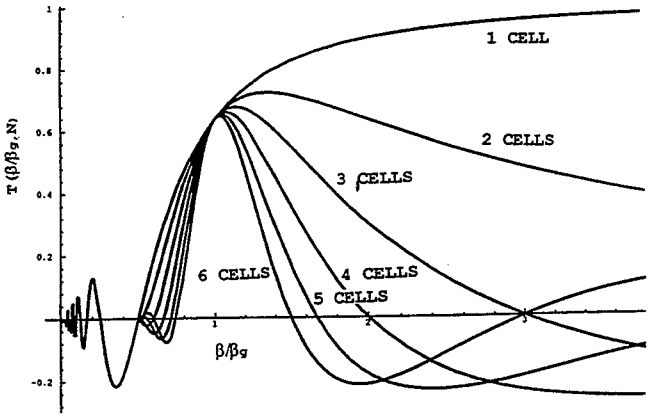

Fig. 1. Transit-time factor from the model versus β/β_G.

The rf power required to accelerate the beam can be expressed as the product of the beam current times the energy gain per cavity:

$$P_C = I\Delta W = IE_a\frac{T(\beta)}{T(\beta_D)}\cos(\phi)N\frac{\beta_G\lambda}{2}. \quad (2)$$

Here, I is the average beam current and E_a is defined in terms of the spatial average of the axial accelerating field E_o and the transit-time factor for the design velocity $T(\beta_D)$ as $E_a = E_o T(\beta_D)$; $T(\beta)$ is the transit-time factor at the reference-particle velocity β; ϕ is the phase of the field when the design particle is at the center of a cavity; and N is the number of cells/cavity. The cell length equals $\beta_G\lambda/2$, where λ is the free-space wavelength. The design velocity β_D is defined as the velocity that gives the maximum transit-time factor. The velocities, β_D and β_G, are nearly, but not exactly, the same due to the gap factor, which increases with increasing particle velocity. This can be seen in Fig. 1. A higher velocity particle spends less time in the gap, experiencing a smaller transit-time reduction. The relation between β_D and β_G

*Work supported by the U. S. Department of Energy

depends on the number of cells/cavity. For a 4-cell cavity, $\beta_D = 1.05\beta_G$.

The transit-time factor decreases as the reference-particle velocity β varies from β_D. In order to efficiently accelerate the beam, we have arbitrarily allowed the transit-time factor to decrease no more than 20% of the maximum value for a given cavity of N cells. Equation 1 can be used to determine the velocity limits for a given constant-β section (all identical cavities) if the number of cells/cavity has been chosen. For a 4-cell cavity, it is found that $T(\beta)/T(\beta_D) = 0.8$ at $\beta/\beta_G = 0.879$ and 1.283. If the beam velocity is specified at either end of the section, β_G, β_D, and the β at the other end of the section can be calculated from these ratios. For our design example with a starting $\beta_{Min} = 0.425$ (98.3 MeV) and using the β/β_G ratios above, $\beta_G = 0.484$, $\beta_D = 0.506$, and $\beta_{Max} = 0.620$ (261 MeV). Iteration for the next section gave a $\beta_G = 0.706$ and $\beta_{Max} = 0.906$ (1276 MeV). Therefore, for our example only two cavity types are required (2 sections). We will call the 100-261 MeV section the medium-β section and the 261-1000 MeV section the high-β section.

The amount of power per cavity available to accelerate the beam is limited by rf power coupler capacity. We have assumed a conservative maximum capacity of 105 kW per coupler and two couplers per cavity (210 kW maximum per cavity). To obtain good power efficiency, it is desirable to have all rf power couplers deliver power at their maximum capacity. Therefore, all cavities in a section will have an identical energy-gain per cavity if E_a is allowed to vary over the section. A 20% variation in E_a over the section will be required to maintain a constant value of $E_o T(\beta)$ over the entire velocity range due to the constraint $T(\beta)/T(\beta_D) \geq 0.8$.

We have used the energy gain per cavity of the high-β section, since it contains the largest number of cavities, to constrain the accelerating gradient throughout the linac. The energy gain per cavity can be calculated using Eqn. 2. For $I = 100$ mA and $P_C = 210$ kW, the energy gain per cavity is 2.10 MeV. For our design example, we have chosen $\phi = -35°$, $N = 4$, and $\lambda = 0.428$ (700 MHz) which results in a value of $E_a T(\beta)/T(\beta_D) = E_o T(\beta) = 4.24$ MV/m. This is a relatively conservative accelerating gradient for superconducting cavities and will be used for both sections of the linac in our example. The energy gain/cavity for the medium-β section is reduced by the ratio of the medium-β to high-β cell lengths and is 1.44 MeV.

Design Algorithm

In order to generate a linac design, a computer design program was written which uses an iterative procedure to determine the required rf field amplitude and injection phase for each cavity such that the desired energy gain per cavity, ΔW, and average synchronous phase is achieved. In order to achieve this, the cavity rf amplitudes must vary as a function of beam energy to compensate for the variation in the transit-time factor.

The algorithm we have used is an iteration procedure which can be used to generate a linac cavity-by-cavity. It assumes that ΔW, β_G, and ϕ are specified, and that $T(\beta)$ can be calculated. A polynomial fit obtained from actual elliptical cavity shapes, developed using the MAFIA codes, was used to specify $T(\beta)$. Initial guesses for the injection phase(ϕ_{in}), at the center of the first gap, and cavity field (E_o) are calculated using the expressions:

$$E_o = \frac{\Delta W}{(N\beta_G\lambda/2)T_{ave}\cos\phi}, \qquad (3)$$

$$\phi_{in} = \phi - \frac{\pi}{2}(N-1)\left(\frac{\beta_G}{\beta_{ave}} - 1\right) \qquad (4)$$

where ϕ is the phase of the field when the design particle is at the center of a cavity (average phase) and β_{ave} is the average velocity calculated using the average beam energy in the cavity, $W_{ave} = W_{in} + 1/2\,\Delta W$. The average of the transit-time factors for the inner and end cells of a cavity, T_{ave}, seen in Eqn. 3, is given by $T_{ave}(\beta) = 1/N\,(2T_{end} + (N-2)T_{inner})$. These transit-time factors differ because of the field leakage at the end cells into the beam pipe due to the large cavity bore. Equation 4 is merely a phase shift from the physical center of the multi-cell cavity back to the center of the first gap seen by the beam.

Next, an integration over all N-cells in the cavity is performed to determine the beam output energy (W_{out}) and phase (ϕ_{out}) using:

$$W_{out} = W_{in} + \sum_{k=1}^{N} E_o T_k(\beta_k)\frac{\beta_G\lambda}{2}\cos\phi_k \qquad (5)$$

and

$$\phi_{out} = \phi_{in} - \sum_{k=1}^{N}\pi\left(1 - \frac{\beta_{ave}}{\beta_k}\right). \qquad (6)$$

The average cavity phase is then calculated from ϕ_{in} and ϕ_{out}, and is compared to the desired average phase. We have required that these two average phases agree to within 0.05°. If not, a new guess for the injection phase is made using $\phi_{in,new} = \phi - 1/2(\phi_{out} - \phi_{in})$, and a new iteration is begun. Once an injection phase for the cavity has been determined, a comparison is also made between the calculated energy gain and the desired energy gain. If the difference in energy gain is greater than 1 keV, a new guess for the cavity field is determined using $E_{o,new} = E_o\,\Delta W_{desired}/\Delta W$, and a new iteration is begun. We have found this algorithm to converge rapidly.

Simulation Results

In order to perform simulations using the results of the design code, a beam dynamics simulation code to model

elliptical superconducting cavities was written. This code is not discussed here, only the simulation results. It should be noted that, the linac example presented here is unoptimized. We have chosen conservative requirements for the various system components, most of which have already been demonstrated in existing accelerators or laboratory tests.

Table 1 gives some of the accelerator parameters. The linac consists of two sections (medium-β and high-β). Each section is composed of identical 4-cell elliptical cavities, with cell lengths equal to $\beta_G\lambda/2$. The β_G- values for the two sections are β_G=0.48 and β_G=0.71, as discussed earlier. A cryostat containing two cavities forms a cryomodule. In this example, transverse focusing is provided by quadrupole doublets between each cryomodule. The power from each klystron would be split among four cavities and fed to each cavity using two antenna-type power couplers, each capable of handling 105 kW.

Table 1 - High-Energy Superconducting Accelerator Parameters

Parameter	
Energy Range (MeV)	100 - 1000
Frequency (MHz)	700
Beam Current (mA)	100
No. of β Sections	2
No. of Cavities	488
No. of Cryostats	244
No. of Klystrons	122
Cavities/Cryostat	2
Cavities/Klystron	4
Cells/Cavity	4
RF Couplers/Cavity	2
RF Power/Klystron (MW)	0.67 (med.-β), 1.0 (high-β)
RF Power/Coupler (kW)	72 (med.-β), 105 (high-β)
Accelerating Field, E_a (MV/m)	4.2-5.3
Average Phase (deg)	-35
Aperture Radius (cm)	5.0 (med.-β), 7.2 (high-β)

Simulation results for the ideal linac show emittance growths from 100-1000 MeV of 25% and 8%, respectively, for the transverse and longitudinal degrees of freedom. We have used the ratio of transverse aperture radius to rms beam size as a figure of merit in our designs. For this example, our simulation results show this ratio ranges from 19 to 26, which is comparable to past results for room-temperature designs.

The large velocity acceptance of these cavities allows operational flexibility. In normal operation, the multi-cell cavities will be operated for a specific energy gain per cavity (medium-β $\Delta W = 1.44$ MeV, high-β $\Delta W = 2.1$ MeV) with an average synchronous phase of -35°. To investigate alternative operating schemes that use the inherent flexibility of a linac built from independently-phased resonators, three examples were simulated. The simulation results are given in Table 2, below. Case 1 assumes that all cavities will be operated at a constant accelerating field of $E_a = 5.3$ MV/m. This is the maximum field under normal operating conditions. In this scheme, the energy gain per cavity is no longer fixed. We have assumed a cavity average synchronous phase of -35°. As can be seen, the beam output energy is raised by 99 MeV. The changes in output beam emittances and ratio of transverse aperture to rms beam size are small. Also shown in Table 2 is the minimum required beam current to produce 100-MW output beam power at 1099 MeV. This example demonstrates an alternative operating scheme which could be used in the event of source output current degradation. In Case 2, the average synchronous phase has been reduced to -25°. As is expected, the output energy is further increased to 1179 MeV. In Case 3, the cavity fields have been increased by 33%. This scheme demonstrates a possible upgrade path, which would require significantly increased power-coupler capabilities and klystron output to produce 130 MW of beam power, without requiring additional accelerating cavities. In the last two schemes, there is a slight degradation in the ratio of transverse aperture to rms beam size. Transverse emittance growth is observed in all cases, which is comparable to the 25% observed for the nominal operating mode. The effects of emittance growth on beam uniformity at a neutron production target have not been studied.

Table 2 - Alternative operating schemes for the high-energy superconducting option. Required beam current is the beam current required to produce a 100-MW beam power.

Case	Output Energy (MeV)	Trans. Emittance Growth	Long. Emittance Growth	Required Beam Current	Aperture Ratio, Med.-β, High-β
1	1099	17%	-5%	91 mA	18, 21
2	1179	32%	98%	85 mA	18, 20
3	1297	19%	-4%	77 mA	17, 20

Experience at operating superconducting accelerator facilities has shown that often there is a large variation in the maximum accelerating gradients achieved in identical multi-cell accelerating cavities. Typically these are $\beta_G = 1$ cavities used to accelerate electron beams. If cavities fail or perform at lower than expected accelerating gradients, the gradients and rf phases in the other cavities are adjusted to compensate and provide the required additional energy gain. A possible solution to increase machine availability is to provide additional accelerating cavities, thus anticipating some fraction of cavity failures. We simulated a case where 5% of the total cavities were failed (every 20th cavity off) with 5% additional cavities added to the high-β section. Simulation results, using a simple algorithm for setting the cavity phases, showed a transmission of 100% with a reduced output beam energy of 993.4 MeV for this case. Small adjustments of the phases should restore the correct final beam energy. The transverse and longitudinal emittances were observed to grow by factors of 2.9 and 6.8, respectively; however, only small reductions in the aperture to rms values were observed.

References

[1] D. K. C. Chan, "Conceptual Design of a Superconducting High Intensity Proton Linac," this conference.